# Heterogeneous integration of evanescently-coupled GaAs-based amplifiers for laser systems emitting in the near-infrared

K. Akritidis,[1,2,4] M. Billet,[1,2] M. Kiewiet,[1,2] J. Fricke,[3] H. Wenzel,[3] J-P. Koester,[3] A. Knigge,[3] P. Neutens,[4] R. Jansen,[4] J. Brouckaert,[4] P. Van Dorpe,[4] M. Weyers[3] and B. Kuyken[1,2]

[1] Photonics Research Group, INTEC Department, Ghent University - imec, 9052 Ghent, Belgium
[2] Center for Nano- and Biophotonics, Ghent University, Belgium
[3] Ferdinand-Braun-Institut (FBH), 12489 Berlin, Germany
[4] IMEC, Kapeldreef 75, 3001 Heverlee, Belgium

*Integrated silicon nitride (SiN) photonic circuits, due to their low loss, CMOS-compatibility and high transparency window, hold great promise for numerous near-infrared (NIR) applications, including optical coherence tomography. Key requirement of these systems is the development of narrow-linewidth integrated lasers emitting in the NIR. Since SiN cannot create gain, the heterogeneous integration of different materials on the platform is required. A promising and versatile technology that enables the latter is micro-transfer printing. Today, two challenges remain. The first involves efficiently coupling light from the passive circuit into the amplifier, for which we propose an evanescent adiabatic coupling scheme, that is alignment-tolerant and coupling-efficient. Due to the high refractive index contrast between the passive circuit and the active device, however, an intermediate layer is required. In this context, we present the design of an adiabatic evanescent coupler using hydrogenated amorphous silicon (a-Si:H) which was engineered for optimized losses. The second challenge involves the transfer printing of amplifiers providing gain in the NIR. As proof of concept, we demonstrate the transfer printing of gallium-arsenide (GaAs)-based amplifiers, compatible with our evanescent-coupling design. These results pave the way towards the realization of evanescently-coupled SiN/GaAs heterogeneous laser systems emitting in the NIR.*

## Introduction

With the emergence of integrated silicon nitride photonics, a powerful, low-loss, passive platform was established enabling on-chip solutions for important fields in the visible to near-infrared domain. These include, among others, atomic physics, biosensing, quantum sciences and medical imaging. An application of particular interest that could benefit from this is optical coherence tomography [1], which to this day relies on expensive bulk opto-mechanical or fiber-based devices. Central to its realization is the development of a widely tunable integrated laser that emits in the near-infrared band. Due to the inability of SiN to create gain, however, the heterogeneous integration of different III/V-based material platforms is required. A versatile and flexible technology that can facilitate this is micro-transfer printing which combines the high throughput of die-to-wafer bonding and the pre-fabrication and testing of flip-chip integration [2]. Due to the high refractive index contrast between the SiN and the III/V, however, using an evanescent field-based adiabatic coupling scheme to directly couple from SiN to III/V is impossible. On the other hand, with butt coupling, in addition to the inherent difficulty to vertically align the integrated layers, which results in a reduced coupling efficiency, etched facets are used which are prone to degradation. By employing instead, a solution based on the addition of an intermediate layer with the appropriate optical properties, an adiabatic facets-free transition with high efficiency and alignment tolerance can be achieved.

In this context, we present an intermediate layer taper design consisting of hydrogenated amorphous silicon (a-Si:H) which was engineered to both tackle the index mismatch and in addition to demonstrate reasonable losses (3 dB/mm at 920 nm). With this design a SiN-III/V transmission of 97% is achieved with good alignment tolerance, obtaining more than 70% efficiency for a maximum misalignment of 500 nm, which is compatible with the state-of-the-art transfer printers. Finally, in this paper we also demonstrate the successful transfer printing of a GaAs-based amplifier on top of the a-Si:H waveguide emitting in the NIR.

## Design

For the adiabatic transition of the mode from SiN to the III/V the phase-matching condition must be satisfied [3]. This means that the effective index of the ground TE mode of the intermediate layer should be equal to the effective index of the ground TE mode of the SiN on one end and to the III/V on the other. With a refractive index of 1.992 for SiN, 3.612 for a-Si:H and 3.2-3.5 for the GaAs-based epi stack, the taper was designed at 920 nm by using a commercial software (Ansys Lumerical MODE). The schematic along with the mode profiles acquired with finite difference eigenmode (FDE) simulations are shown in Figure 1.

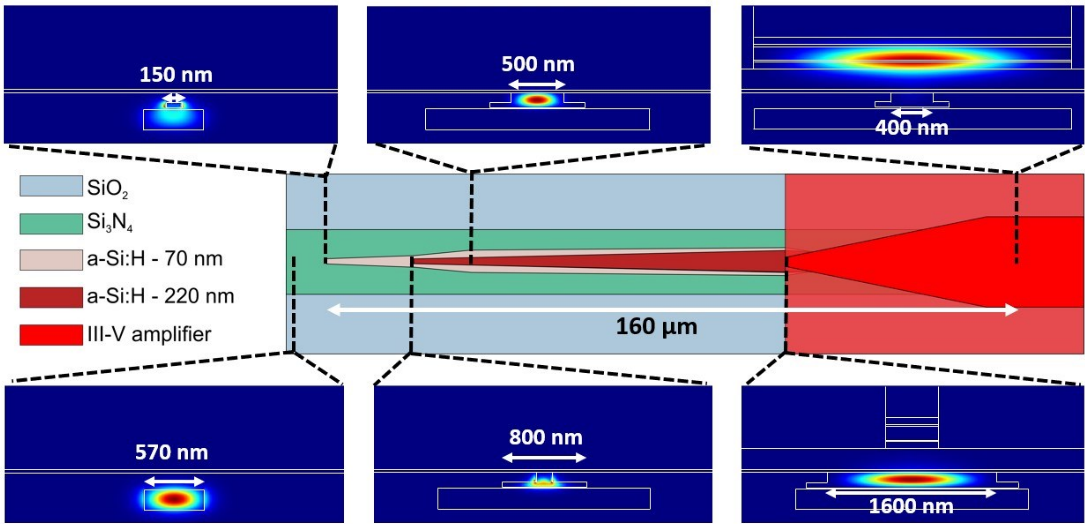


*Figure 1: Schematic depiction of the various tapers for the transition of the mode from SiN towards the GaAs-based amplifier. Critical geometrical dimensions along with FDE results are shown as well.*

In the simulation a very thin cladding of 20 nm benzocyclobutene (BCB) is taken into account. Its role is to facilitate the transfer printing of the amplifier acting as an adhesion layer. By running eigenmode expansion (EME) simulations the transmission to the fundamental TE mode of the III/V-based amplifier is calculated. A transmission of 97% at 920 nm is found by assuming zero misalignment. In reality, however, misalignment during the transfer printing is expected which for the state-of-the-art printers is $\pm\, 0.5\ um$.

By taking this variation into account, a simulated transmission of over 70% is found for a maximum misalignment of 0.5 µm (Figure 2).

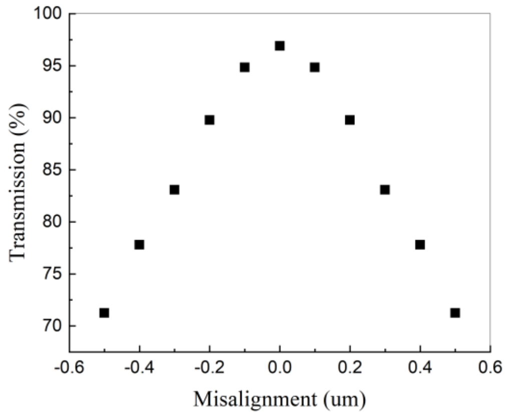


*Figure 2: Simulated transmission with respect to misalignment during transfer printing.*

## Fabrication

For the transfer printing of the amplifiers, first the source wafer was processed for the fabrication of micro-transfer-printing-compatible coupons. Details of the transfer printing technology and the coupons' general structure can be found in [2, 4]. After the preparation of the source wafer, the target substrate was prepared by patterning structures including waveguides, tapers and grating couplers on a 200 nm a-Si:H layer using electron beam lithography. The 20 nm deviation from the optimal thickness is expected to result in an additional 0.4 transition loss.

Following the patterning of the waveguides, we spin-coated a thin BCB layer of 20 nm and proceeded with the heterogeneous integration of the amplifiers with the target heated to 75 °C. As the coupons were approximately $1400 \times 50$ µm$^2$, we used a polydimethylsiloxaan (PDMS) stamp of $1500 \times 80$ µm$^2$. In Figure 3(a), we show a microscope picture of the bottom side of the picked coupon. The smooth and clean bottom surface both indicate the success of the picking phase. After the transfer printing was complete, BCB curing at 280 °C for a few hours took place, followed by photolithography and metal deposition to create the contact pads. After lift-off the sample was ready for measurements. An image of the printed amplifier on the target prior to the metallization of the contact pads is shown in Figure 3(b).

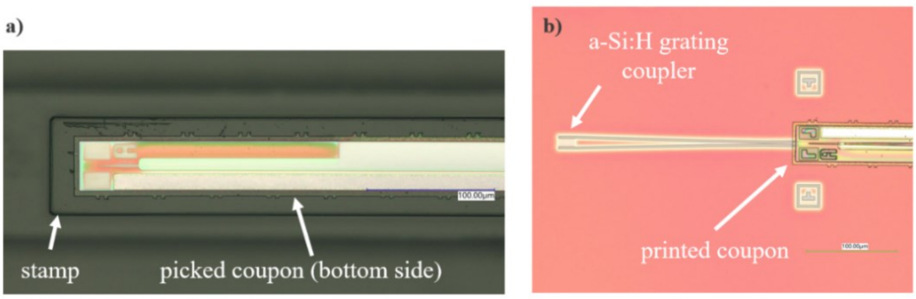


*Figure 3: (a) The bottom side of the picked coupon as held by the PDMS stamp. The bottom side is clean and shows no topography. (b) The printed amplifier on top of the a-Si:H waveguide before the metallization of the contact pads.*

## Results

To demonstrate the operation of the printed amplifiers, we measured the power of the amplified spontaneous emission that was coupled into the a-Si:H waveguide and out through the grating coupler with a powermeter, by applying a DC bias via probes connected to a power supply (Figure 4(a)). The power is shown to saturate at around 60 mA with a value of -50 dBm. With a 15 dB insertion loss for the grating coupler and 0.5 dB for the a-Si:H waveguide propagation losses, the generated power coupled to the waveguide is estimated to be around -34 dBm. In addition, by using an optical spectrum analyzer we extracted the power spectral density for different driving currents as shown in Figure 4(b). The spectra are centered around 925 nm with a FWHM (full width at half maximum) optical bandwidth of approximately 40 nm. The calculated bandwidth however does not necessarily depict the maximum optical bandwidth of the amplifier, as the measurements are filtered by the transmission spectrum of the a-Si:H grating coupler.

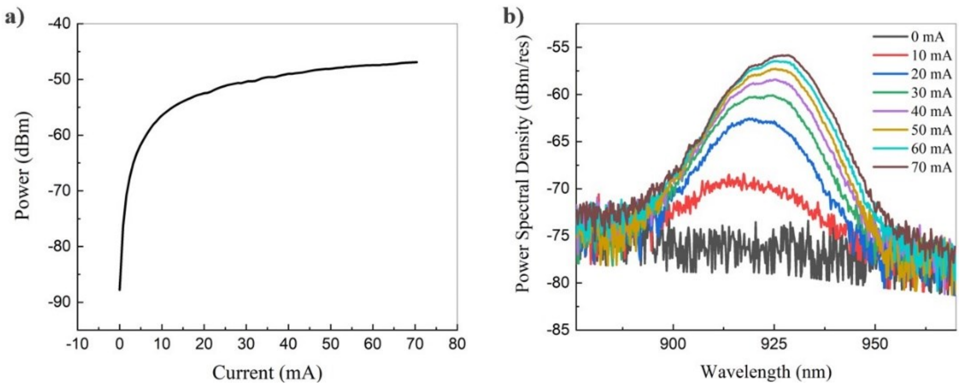


*Figure 4: (a) Power-current measurements. (b) Power spectral density for different driving currents.*

## Conclusion

In this work we showed a design based on a-Si:H as the intermediate layer in order to transition adiabatically from SiN towards the III/V. Moreover, we demonstrated the successful heterogeneous integration of a GaAs-based amplifier by measuring the amplified spontaneous emission through the a-Si:H grating coupler. The power spectra were centered at 925 nm with a FWHM optical bandwidth of 40 nm. These results prove not only that the transfer printing along with the a-Si:H/III-V coupling works, but also that we have light emission in the wavelength range of interest. The next step is to include the passive SiN circuitry and use the optimal a-Si:H taper design, in order to develop fully heterogeneously integrated evanescently-coupled laser systems emitting in the NIR.

## References

[1] E.A. Rank et al., “Toward optical coherence tomography on a chip: in vivo three-dimensional human retinal imaging using photonic integrated circuit-based arrayed waveguide gratings,” Light Science & Applications, vol. 10, no. 6, 2021

[2] G. Roelkens et al., “Micro-Transfer Printing for Heterogeneous Si Photonic Integrated Circuits,” IEEE Journal of Selected Topics in Quantum Electronics, vol. 29, no. 3: Photon. Elec. Co-Inte. and Adv. Trans. Print., pp. 1–14, 2023

[3] Yuting Shi et al., "Novel adiabatic coupler for III-V nano-ridge laser grown on a Si photonics platform," Opt. Express 27, 37781-37794, 2019

[4] Jing Zhang et al., "III-V-on-Si photonic integrated circuits realized using micro-transfer-printing," APL Photonics, 2019

## Posters (odd numbers):

1. Thermal design considerations for vertical integration of InP nanophotonic membrane devices with InP electronics
Salim Abdi

3. Using Optical Ring Resonators for True-Time Delay: Investigating the Required Delay Bandwidth
Bart Bas

5. Design of C-band electro-absorption modulator/DFB laser monolithically integrated with selective area growth on InP membrane
Zhaowei Chen

7. Parity-time symmetric waveguides coupled through chiral materials
Alice De Corte

9. UV Photonic integrated Circuits for Structured Illumination Microscopy with High Optical Throughput
Shiqi Fang

11. Electrochemical etching – a way to enable transfer-printing of III-nitride devices
Natalia Fiuczek

13. Equivalent circuit modelling of high-speed coplanar strip InP-based Mach-Zehnder phase modulators
James Hillier

15. Simulations of a sub-kilohertz linewidth laser in monolithic indium phosphide
Julian Konig

17. Finite Element Modelling of Liquid Crystal Orientation and Its Applications in a Tunable Bimodal Periodic Waveguide
Jiayi Liu

19. Toward Speckle-free Laser Engines on Chip for AR/VR displays
Dennis Maes

21. A computationally efficient tool for calculating the field in a multi-mode fiber

## Posters (even numbers):

2. Heterogeneous integration of evanescently-coupled GaAs-based amplifiers for laser systems emitting in the near-infrared
Konstantinos Akritidis

4. Ultra flat butt-joint interface in InGaAsP-based active/passive waveguides
Zhaowei Chen

6. Dispersion adapted Nonlinear Schrödinger equation to simulate Kerr effects inside a Bragg grating
Timothé David

8. Characterization of optical waveguides engraved in silica planar substrates with a femtosecond laser process
Tunon De Lara

10. Comparison of thermo-optic phase shifters in silicon platforms
Yuxi Fang

12. VCSEL wavelength tunability using controlled mechanical strain
Salah Guessoum

14. Numerical comparison of sensing performance of a microring resonator and Mach-Zehnder interferometer in Al2O3
Bram Kok

16. Implementation and Comparison of Dilithium/Kyber and Falcon/Kyber PQC software stack on data processing units
Daniel Christian Lawo

18. Microscopy on a Chip
Chunyu Lu

20. Process flow optimization for a fabrication-friendly polarization converter design on the monolithic integration generic InP platform
Kolsoom Mehrabi

22. Dissipative coupling between ring resonators for large area, single mode lasing at